Cooperative Topology Sensing of Wireless Networks With Distributed Sensors

Zitong Liu, Guoru Ding, *Senior Member, IEEE*, Zheng Wang, *Member, IEEE*, Shilian Zheng, *Member, IEEE*, Jiachen Sun, and Qihui Wu, *Senior Member, IEEE*

***Abstract*—As a key technology of network inference, topology sensing plays an important role in understanding, explaining and predicting network behavior. Majority of existing studies focus on topology inference with complete and perfect observations, which is mainly suitable for wired networks rather than wireless networks with kinds of channel randomness and uncertainty. This article investigates the issue of topology sensing of wireless networks with distributed sensors to handle the situation of limited and unreliable information, which include a time series of the signal presence instants and the corresponding transmitter identification. Firstly, a cooperative topology sensing framework is developed to exploit multi-sensor spatial diversity for coping with wireless randomness. Then, based on the observation that in wireless networks, events at one node are likely to induce a response at some other node in the form of for example an acknowledgement message or a forwarding action, we formulate the communication events among multiple wireless transceivers as a multi-dimensional Hawkes process. Further, we propose and analyze four cooperative topology sensing schemes with distributed sensors from the perspective of hard fusion and soft fusion, respectively. Moreover, simulation results show that the signal power and the event number have a great influence on sensing accuracy and cooperative topology sensing is an effective measure to deal with the issues of wireless channel randomness.**

***Index Terms*—Network inference, topology sensing, spatial diversity, Hawkes process, data fusion.**

I. Introduction

A. Background and Motivation

With the popularization of complex systems, the science of networked interactions has become a major tool to understand, explain and predict network behavior [1]. Besides the well-known studies on statistical inference of interactions in human social networks [2], brain neural networks [3], financial markets [4] and genomics [5], the research on the interaction in communication networks has also received increasing attention during the past few years.

A promising technique in understanding communication network structure is the identification of the underlying topology via sensing and inference [6], [7]. Most of existing studies explicitly or implicitly assume that the network interaction information used for topology inference is perfect. However, in wireless networks, ubiquitous randomness and uncertainty makes the information noisy and unreliable. Moreover, the information for network topology inference is generally limited due to the lack of cooperation between the target wireless network and the sensor network. These observations motivate us in this article to investigate the issue of topology sensing of wireless networks with limited and unreliable information.

B. Related Work

Generally, the existing studies on topology sensing can be grouped into two categories: In-network sensing and out-network sensing. The former refers to the case that the sensor nodes are part of the sensed network and can infer the network topology structure based on in-network message exchange. Differently, out-network topology sensing refers to the case that the sensor nodes do not belong to the network to be sensed and can only infer the network topology based on passive observations from an outsider perspective. The early topology sensing works mainly focus on in-network sensing, which are implemented by routing information exchange [8], [9]. In [8], a network topology discovery algorithm based on simple network management protocol was proposed. In [9], Shaikh *et al.* proposed an open shortest path first protocol to construct and monitor the network topology.

As mentioned in [10], the research of out-network topology sensing has recently received increasing attention [11]–[16]. Dynamic causality model was proposed in [11] to model interactions among neuronal populations, which can be extended to the field of communication. Granger causality was used in [12], [13] to model the response mechanism of common

Manuscript received November 3, 2019; revised May 26, 2020 and July 15, 2020; accepted August 17, 2020. Date of publication August 26, 2020; date of current version June 9, 2021. This work is supported by the National Natural Science Foundation of China (No. 61871398, No. 61931011, No. 61631020, No. 61801216), the Natural Science Foundation for Distinguished Young Scholars of Jiangsu Province (No. BK20190030), the Natural Science Foundation of Jiangsu Province (No. BK20180420), the open research fund of Key Laboratory of Dynamic Cognitive System of Electromagnetic Spectrum Space (Nanjing Univ. Aeronaut. Astronaut.), Ministry of Industry and Information Technology, Nanjing, China (No. KF20181913). The associate editor coordinating the review of this article and approving it for publication was K. Choi. *(Corresponding authors: Guoru Ding; Qihui Wu.)*

Zitong Liu, Zheng Wang, and Qihui Wu are with the Key Laboratory of Dynamic Cognitive System of Electro-Magnetic Spectrum Space, Nanjing University of Aeronautics and Astronautics, Ministry of Industry and Information Technology, Nanjing 211106, China (e-mail: zt_liu@126.com; z.wang@ieee.org; wuqihui2014@sina.com).

Guoru Ding and Jiachen Sun are with the College of Communications Engineering, Army Engineering University, Nanjing 210007, China (e-mail: dr.guoru.ding@ieee.org; sun_jiachen@outlook.com).

Shilian Zheng is with the No. 011 Research Center, Science and Technology on Communication Information Security Control Laboratory, Jiaxing 314033, China (e-mail: lianshizheng@126.com).

Digital Object Identifier 10.1109/TCCN.2020.3019601

communication protocols and learn the topology structure of time-multiplexed communication networks, where simulation demonstrated that this method can infer the directed data flow in an Ad-hoc network. The authors in [14] modeled the information transmission as a Hawkes process by leveraging the reasonable assumption of communication equivalence. On the basis of [14], the low cost paths for acyclic graphs algorithm was further proposed in [15] to discover event chains. The authors in [16] leveraged transfer entropy as a metric for quantifying the strength of the automatic repeat request mechanisms in next-hop routing links.

Topology sensing has also been studied in graph signal processing in recent years. The authors in [17] surveyed solutions to the problem of graph learning, including classical viewpoints from statistics and physics, and more recent approaches that adopt a graph signal processing perspective. In [18], the authors offered an overview of graph-learning methods by using information available from graph signals to infer the underlying graph topology. The authors in [19] proposed a method that finds a block sparse representation of the data by associating a graph, whose Laplacian matrix admits the sparsifying dictionary as its eigenvectors. The work in [20] put forth a joint diagonalization-based approach to directed network topology inference, in which novel identifiability guarantees are derived regardless of the exogenous inputs or their statistics. Although this kind of researches focus on the out-network topology inference, the methods in these works are always applied to the fields of neuroscience, social network and so on. So far, the mapping between the communication behavior and the graph signal processing has been rarely studied.

Through the above research, it is found that the existing studies mainly have two limitations. Firstly, the majority of studies focus on topology inference with complete and perfect observations, which is mainly suitable for wired networks like Internet, however, not for wireless networks with kinds of channel randomness and uncertainty. Secondly, they consider that there is only one sensor involved in the topology sensing process and the potential of employing multiple sensors collaboratively perform network topology sensing is not well explored. In response to these observations, this article investigates the issue of topology sensing of wireless networks with distributed sensors to handle the situation of limited and unreliable information by exploiting user cooperation diversity [21], [22].

Notably, topology sensing is similar to spectrum sensing from a view of sensing, but the two processes are not exactly the same because of the different tasks. For example, the key task of spectrum sensing is to determine the presence of a transmission, which is a signal detection problem [23], [24]. Differently, the key task of topology sensing is to infer the connection relationship between several nodes, which is a statistical inference problem. To some extent, topology sensing can be regarded as an extension of spectrum sensing.

C. Contributions

The main contributions of this article are summarized as follows:

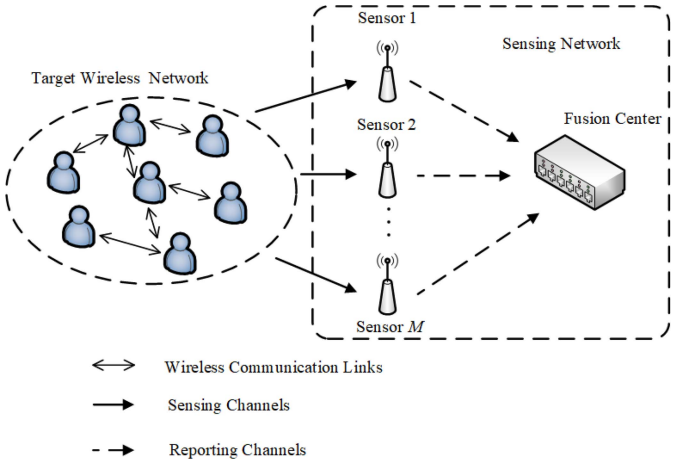

Fig. 1. The system model of topology sensing with distributed sensors.

- We develop a cooperative topology sensing framework based on multi-sensor with limited and unreliable information to exploit multi-sensor spatial diversity for coping with wireless randomness.
- We propose and analyze four cooperative topology sensing schemes with multiple distributed sensors from the perspective of hard fusion and soft fusion, respectively. Specifically, the schemes include soft fusion of signal powers (SFSP), hard fusion of signal detections (HFSD), soft fusion of influence matrixes (SFIM) and hard fusion of influence matrixes (HFIM), respectively.
- We present in-depth simulations under various parameter configurations, which suggest that the signal transmit power and event number have a great influence on sensing accuracy. It is also suggested that cooperative topology sensing is an effective measure to deal with the issues of wireless channel randomness.

The remainder of this article is organized as follows. In Section II, the cooperative topology sensing framework and the problem of interest are introduced. Then, four multi-sensor cooperative topology sensing schemes are proposed in Section III. Section IV presents the simulations and discussions of schemes' performance. Finally, Section V draws conclusions.

II. System Model and Problem Formulation

A. Cooperative Topology Sensing Model

A cooperative topology sensing model shown in Fig. 1 is considered in this article, which consists of a target wireless network and a sensing network. In the target wireless network, N_{node} nodes exchange data with each other through wireless communication links, in a distributed time division multiple access manner. In the sensing network, there are M distributed sensors and a fusion center (FC) working together. During a sensing period, distributed sensors detect the presence of a signal independently through sensing channels. If the signal is present, sensors identify the transmitter of the signal and record the information of the transmitter identification and the presence time of the signal. After a sensing

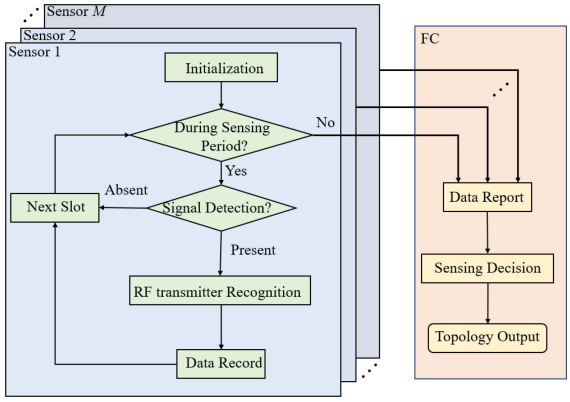

Fig. 2. The workflow of cooperative topology sensing.

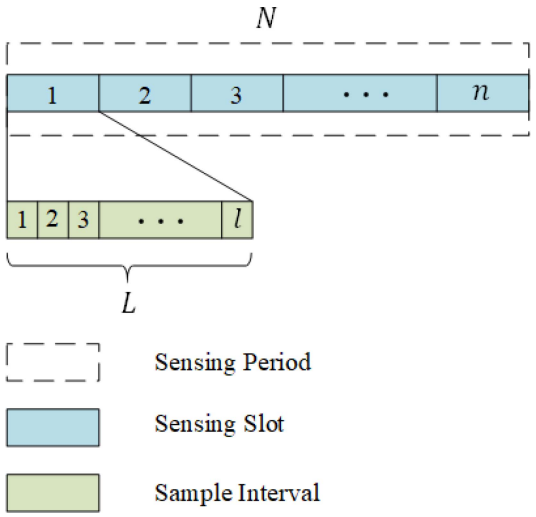

Fig. 3. The illustrative relation of sensing period, sensing slot, and sample interval in once topology sensing process.

period, distributed sensors send sensing data to the FC through reporting channels. Then, FC makes global decisions to infer the target network topology.

As shown in Fig. 2, for each individual sensor, there are mainly three steps involved in the overall topology sensing process: signal detection [25], radio frequency (RF) transmitter recognition [26]–[29] and topology sensing decision, in which the data from signal detection and RF transmitter recognition is the evidence of topology sensing decision. This suggests that there may be two sources of unreliable information: 1) signal detection error: The sensor will be affected by the wireless environment and noise so as to detect the signal erroneously. 2) RF transmitter recognition error: The sensor may wrongly identify the source of the signal. In this article, we focus on the error in the signal detection and model it in the next section. The impact of RF transmitter recognition error will be shown in Fig. 18 of Section IV.

B. Signal Detection Model

Considering the cooperative topology sensing problem in Fig. 1, there are three kinds of wireless channels in this system, communication links between network nodes in the target wireless network, sensing channels between the target wireless network and the distributed sensors, and reporting channels between the distributed sensors and the FC. Notably, the sensing channels is one kind of inter-network channels while the rest two kinds of channels are in-network channels. Thus, in this work, we focus on the case that the sensing channels are of randomness and uncertainty due to the lack of cooperation between the target wireless network and the sensor network.

In order to detect signal energy clearly, multi-sampling in a slot is a common method. The relation among sensing period, sensing slot and sample interval is shown in Fig. 3. It means that there are *L* samples in a slot for once signal detection and the data in a period which includes *N* slots is used for once topology inference.

In this article, we consider that the signal detection error comes from the sensing channel. The signal detection is essentially a binary hypothesis-testing problem

$$\begin{aligned} H_0 &: \text{ Signal is absent} \\ H_1 &: \text{ Signal is present.} \end{aligned}$$

The correct detection probability given by $P_d = P_r\{H_1|H_1\}$, the missed detection probability given by $P_m = P_r\{H_0|H_1\}$, the correct non-detection probability $P_n = P_r\{H_0|H_0\}$ and the false alarm probability given by $P_f = P_r\{H_1|H_0\}$ are the key metrics. The signal detection problem is to decide between the following two hypotheses [30]:

$$y^{(j)}(l) = \begin{cases} \varepsilon^{(j)}(l), l = 1, \ldots, L, & H_0 \\ \sqrt{P_r^{(j)}} x^{(i)}(l) + \varepsilon^{(j)}(l), l = 1, \ldots, L, & H_1 \end{cases} \tag{1}$$

in which *L* is the total number of samples in a sensing slot, $P_r^{(j)}$ is the signal power that received by *j*th sensor, $x^{(i)}(l)$ is the signal from the *i*th node in the *l*th received sampling signal, $\varepsilon^{(j)}(l)$ is the additive white Gaussian noise at the *j*th sensor in the *l*th received sampling signal, and $y^{(j)}(l)$ is the signal detected by the *j*th sensor in the *l*th received sampling signal ($i \in [1, N_{node}], j \in [1, M]$).

Therefore, the *j*th sensor in the *n*th slot with *L* signal sampling for energy detection, the test statistic is:

$$E^{(j)}(n) = \frac{1}{L} \sum_{l=1}^{L} \left[y^{(j)}(l) \right]^2. \tag{2}$$

According to the central limit theorem (CLT), when the sample number is sufficiently large, $E^{(j)}(n)$ is approximated as a Gaussian random variable under both hypotheses H_0 and H_1 in the *n*th sensing slot [31], [32]

$$E^{(j)}(n) \sim \begin{cases} N\left(\delta_0, \sigma_0^2\right), & H_0 \\ N\left(\delta_1(d_{ij}), \sigma_1^2(d_{ij})\right), & H_1. \end{cases} \tag{3}$$

where

$$\begin{cases} \delta_0 = \sigma_n^2, \\ \sigma_0^2 = 2\sigma_n^4 / L, \\ \delta_1(d_{ij}) = (1 + \xi_{ij})\sigma_n^2 = (1 + \xi_{ij})\delta_0, \\ \sigma_1^2(d_{ij}) = 2(1 + 2\xi_{ij})\sigma_n^4 / L = (1 + 2\xi_{ij})\sigma_0^2 \end{cases} \tag{4}$$

$\xi_{ij} = P_r^j / \sigma_n^2$ is the received signal to noise ratio (SNR) of the *j*th sensor from *i*th node.

C. Problem Formulation

Now, we formulate the communication events among multiple wireless transceivers as a multi-dimensional Hawkes process based on the observation that events at one node are likely to induce a response at some other nodes in the form of for example an acknowledgement message or a forwarding action in wireless networks. The Hawkes process was first proposed by Hawkes [33] in 1971, which is a good model for describing the aggregation phenomenon of event arrival time. The model was first used in earthquake research [34] and has also attracted wide attention in the financial field because its "self-triggering" nature fits well with the dynamic process of asset prices [35]. In recent years, Hawkes process has begun to emerge in social relation inference [36]. Hawkes process is a point process which depends on autoregressive past events. Its main idea is that the transmission rate of an event at any time is a function of the recent events in the process [15]. In the time point process, each observed point t_i is a basic event that occurs in the point process. That is to say, the sequence $S = \{t_i | i \in Z_+\}$ are generated by a time point process. Defining $N(t, t')$ as the number of points observed during (t, t') and $\Gamma(t) = E[N(0, t)]$ as the expected value of the number of points in the interval, the conditional intensity function (CIF) of the point process is

$$\lambda(t) = \frac{d}{dt} E[N(0,t)] = \frac{d}{dt}\Gamma(t). \tag{5}$$

Hawkes process is a kind of point process with

$$\lambda(t) = \mu(t) + A \sum_{k=1}^{K} \gamma(t - t_k). \tag{6}$$

What is different from the existing studies [11]–[16] is that we divide time into slots, which makes the continuous data become discrete data. It makes the data not conform to any kind of prior distribution. For an event, in a case which has given n_k, the transmission rate of the event is

$$\lambda(n) = \mu(n) + A \sum_{k=1}^{K} \gamma(n - n_k). \tag{7}$$

The parameter $\mu(n) \geq 0$ is the basic rate of the event or the rate of innovation; the parameter $A \geq 0$ indicates the degree of self-motivation of the event, namely, how much influence the event at slot n_k has on the occurrence of the event at slot n, so we can call it the self-motivation matrix; the kernel function $\gamma(n)$ represents the time relationship between the events, which is known, causal, non-negative and additive.

This model can be extended to process containing multiple subprocesses, where the transmission rate of one subprocess is affected not only by its own behavior, but also by the behaviors of other subprocesses. Consequently, we apply the multi-dimensional Hawkes process [14] to model the communication process in the target wireless networks, and regard the transmission behavior of each node in the network as a subprocess. For a process with Z subprocesses, the CIF of the ith subprocess can be given as

$$\lambda_i(n) = \mu_i + \sum_{j=1}^{Z} A_{ij} \sum_{k_j \in K_j} \gamma\Big(n - n_{k_j}\Big), \tag{8}$$

in which K_j represents the event set in jth subprocess, μ_i represents the basic rate of the ith subprocess, A_{ij} quantifies how much the ith subprocess reacts to jth subprocess. $A_{ij} = 0$ represents the case that the occurrence of the jth subprocess has no effect on the ith subprocess and $A_{ij} > 0$ denotes that the occurrence of the jth subprocess will lead to the temporary increase of the occurrence probability of the ith subprocess. We call $\mathbf{A}$ the influence matrix or topology connectivity matrix.

Here we use the maximum likelihood estimation method to determine μ_i and A_{ij} in $n \in [0, N]$, so the negative log-likelihood function of the ith subprocess is given by [37]

$$\mathcal{L}_i(\mu, A) = \int_0^N \lambda_i(n) \mathrm{d}n - \sum_{k_i \in K_i} \log \lambda_i\big(n_{k_i}\big). \tag{9}$$

Therefore, the negative log-likelihood function of all subprocesses combined is simply

$$\mathcal{L}(\mu, \mathbf{A}) = \sum_i \mathcal{L}_i(\mu, A). \tag{10}$$

Then the parameters μ and A, which can be obtained by minimizing the above equation, are given by

$$[\mu, \mathbf{A}] = \underset{\mu, \mathbf{A}}{\operatorname{argmin}} \mathcal{L}(\mu, \mathbf{A}). \tag{11}$$

There are $N(N + 1)$ parameters in the above equation, which is difficult to optimization directly. Since each likelihood depends on only an isolated subset of the parameters, each term can be optimized individually. The detailed solution of equation (11) is given in Appendix A. When given the influence matrix $\mathbf{A}$, we can get the connected relationship of the network nodes.

III. Cooperative Topology Sensing Based on Distributed Sensors

In this section, to exploit multi-sensor spatial diversity for coping with wireless randomness, we propose and analyze four cooperative topology sensing schemes with multiple distributed sensors from the perspective of hard fusion and soft fusion, respectively.

A. Cooperative Topology Sensing Scheme

It is far from enough to use the Hawkes process to deal with the limited and unreliable information. Not only the influence of the environmental noise, but also the limitation of the model itself indicates that further processing of the influence matrix is necessary.

Considering the situation shown in Fig. 4(a), the node a can send data to the node c through the node b. In this case, the node a can send data to the node c, but a is not connected with c so that $A_{ac} = 0$ will be present theoretically. However, the case that $A_{ac} > 0$ does exist in practice. It is because that

Algorithm 1 Cooperative Topology Inference Algorithm Based on Hawkes Process

Input: The number of nodes in the network, N_{node}; The set of events (the source node ID), $\mathbf{E_{node}}$; The set of slots in which there is a signal sent, $\mathbf{E_{slot}}$; The influence matrix threshold, α; The maximum number of relative slots, N_{max}.

Output: Recovered influence matrix, $\mathbf{A}$;

1: Initialize μ, $\mathbf{A}$
2: Sort $\mathbf{E_{node}}$ and $\mathbf{E_{slot}}$;
3: **for** each $i \in [1, N_{node}]$ **do**
4: $index = find(\mathbf{E_{node}} == i)$
5: Find set $\mathbf{K_i}$ such that $\mathbf{E_{slot}^{index}} - \mathbf{E_{slot}^{K_i}} \leq N_{max}$
6: Calculate $\sum_{k_i \in \mathbf{K_i}} \gamma(n - n_k)$
7: $[\mu, \mathbf{A}] = \underset{\mu,\mathbf{A}}{\operatorname{argmin}} \mathcal{L}(\mu, \mathbf{A})$ where
8: $\mathcal{L}_i(\mu, A) = \int_0^N \lambda_i(n)\mathrm{d}n - \sum_{k_i \in K_i} \log \lambda_i(n_{k_i})$
9: **end for**
10: **for** each $i, j \in [1, N_{node}]$ **do**
11: **if** $\mathbf{A_{ij}} < \alpha$ **then**
12: $\mathbf{A_{ij}} = 0$
13: **end if**
14: **end for**
15: **for** each $i \in [1, N_{node}]$ **do**
16: **for** each $j \in [i, N_{node}]$ **do**
17: $A_{ij} = (A_{ij} + A_{ji})/2$
18: $A_{ji} = A_{ij}$
19: **end for**
20: **end for**
21: **for** each $i, j \in [1, N_{node}]$ **do**
22: **if** $\mathbf{A_{ij}} > 0$ **then**
23: $\mathbf{A_{ij}} = 1$
24: **end if**
25: **end for**

a send data may increase the probability of c sending data, which is the same as the main idea of Hawkes process. That is to say, $A_{ac} > 0$ can represent the case that a and c are related but not connected directly. Therefore, it is necessary to set a positive threshold α to eliminate redundant links. For threshold setting, we adopt a heuristic method: a low threshold will be set when the goal of the algorithm is to find all the communication links and a high threshold will be set when the goal of the algorithm is to find the key communication links.

Consider another problem in the situation shown in Fig. 4(a). Directivity of communication links is not considered in this article, that is if a can send data to b, b can send data to a as well, which represented in influence matrix is $A_{ij} = A_{ji}$. However, because of the statistical properties of Hawkes process, $A_{ij} \neq A_{ji}$ will be present if the frequency of information transfers between nodes are different. In some networks, different link frequencies are common to see due to the different node levels, which will affect topology inference. Therefore, by combining the A_{ij} and A_{ji} to measure the connectivity between two nodes, matrix symmetry is also indispensable in order to solve this problem. The rule of matrix

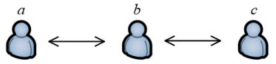

(a) The situation that the node a can send data to the node c through the node b.

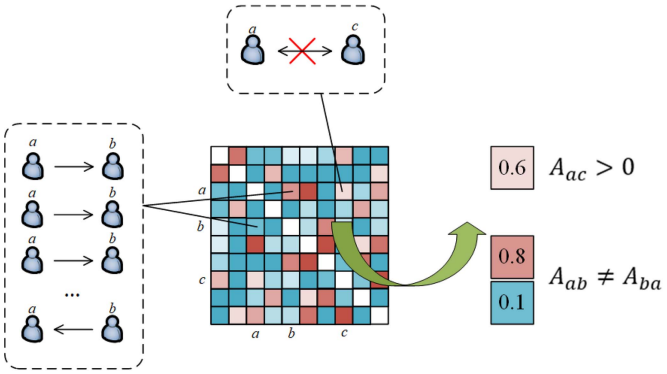

(b) The schematic of two error cases.

Fig. 4. An illustrative example of the situation that Hawkes process cannot deal with.

symmetry can be represented as

$$A_{ij} = (A_{ij} + A_{ji})/2. \tag{12}$$

The above two situations are explained in Fig. 4(b) in which the red represents the large value of A_{ij} and the blue represents the small value of A_{ij}. What cannot be ignored is that the A_{ij} is still a continuous value. Therefore, the last step of the scheme is the binary operation, which is the final decision on whether two nodes are connected or not.

After several attempts, the topology inference process in the cooperative topology sensing scheme is summarized in **Algorithm 1**. The main components of the algorithm are: Hawkes process parameters determination (line 2-9), influence matrix screening and binarization (line 10-26). In terms of the specific fusion method, four types of fusion methods from the perspective of hard fusion and soft fusion are shown in Fig. 5, respectively, which are:

- Soft fusion of signal powers (SFSP): Soft fusion based on global topology inference with local soft signal powers.
- Hard fusion of signal detections (HFSD): Hard fusion based on global topology inference with local binary signal detections.
- Soft fusion of influence matrixes (SFIM): Soft fusion based on global topology decision with local topology inference results, soft influence matrix.
- Hard fusion of influence matrixes (HFIM): Hard fusion based on global integration with local topology decision results, binary influence matrix.

B. Soft Fusion of Signal Powers

The first fusion method with cooperative topology sensing to be considered is based on the fusion of signal powers, which is shown in Fig. 5(a). In this method, the distributed sensors report the collected signal powers to the FC without making

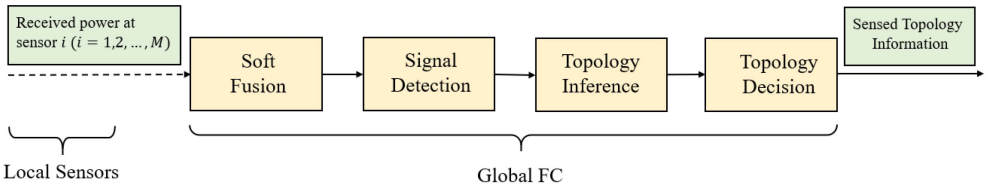

(a) Soft fusion based on global topology inference with local soft signal powers, named soft fusion of signal powers (SFSP)

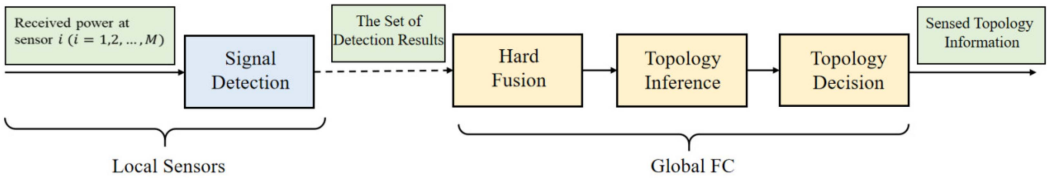

(b) Hard fusion based on global topology inference with local binary signal detections, named hard fusion of signal detections (HFSD)

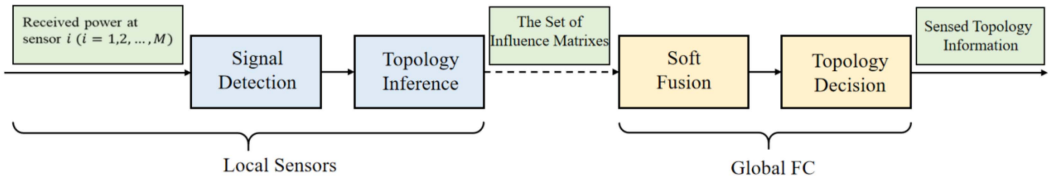

(c) Soft fusion based on global topology decision with local topology inference results, soft influence matrix, named soft fusion of influence matrix (SFIM)

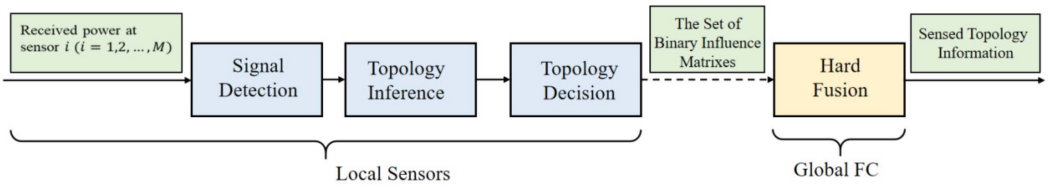

(d) Hard fusion based on global integration with local topology decision results, binary influence matrix, named hard fusion of influence matrix (HFIM)

Fig. 5. The four data fusion frameworks with multi-sensor cooperative topology sensing.

any local decisions. Then, FC fuses the signal powers reported by distributed sensors to detect whether the signal is present. Finally, the FC uses the fused data to make topology inference.

The fusion of signal powers is a kind of soft fusion, which is the fusion of data that typically are real number in nature [38]. Considering the simple equal gain combination, global signal power at this point can be represented by the following equation

$$E(n) = \frac{1}{M}\sum_{j=1}^{M} E^{(j)}(n), \tag{13}$$

where $E^{(j)}(n)$ is the received signal power of the *j*th sensor in the *n*th slot. In this case, the binary hypothesis-testing problem can be described as follows:

$$E(n)\begin{cases} < \zeta, & \text{Decide } H_0 \\ \geq \zeta, & \text{Decide } H_1 \end{cases} \tag{14}$$

After judging whether the signal is present or not, the information of the existing signal is left as the original data of topology inference.

C. Hard Fusion of Signal Detections

Another fusion method with cooperative topology sensing is based on the fusion of signal detections, which is shown in Fig. 5(b). In this method, the distributed sensors report the set of detection result (the sender and slots of signal transmission) to the FC, which integrates data by leveraging the fusion rules and then carries out topology inference algorithm based on Hawkes process to obtain the final influence matrix.

The fusion of signal detections is a kind of hard fusion, which is the fusion of data that objective in nature [38]. Choosing an effective fusion criterion is the core of distributed sensor networks, and there are many common data fusion criterions such as Bayesian criterion [39], Neyman-Pearson

criterion [40], minimum total error probability criterion, minimax criterion and so on. Bayesian criterion may be more familiar with scholars, which making decision by maximizing the posterior probability, however, the prior information $P(H_0)$ and $P(H_1)$ must be available in this situation. The Neyman-Pearson criterion can be used when there is no prior information, which means that maximize the correct detection probability subject to a constraint on the false alarm probability certain, or minimize the false alarm probability subject to a constraint on the correct detection probability certain. Therefore, the correct detection probability and false alarm probability of the *j*th sensor in the *n*th slot are given respectively by

$$\begin{aligned} P_{dj}(n) &= P(u=1|H_1) = P\Big(E^{(j)}(n) \geq \lambda | H_1\Big) \\ P_{fj}(n) &= P(u=1|H_0) = P\Big(E^{(j)}(n) \geq \lambda | H_0\Big), \end{aligned} \quad (15)$$

where λ is the threshold of local signal detection, $u = 1$ donates the decision that signal is detected and data will be recorded. Correspondingly, $u = 0$ donates the case that signal is not detected and data will be discarded. Likelihood ratio test (LRT) [41], [42], the evidence of data fusion, is given as follows:

$$\Lambda_n(\mathbf{u}) \begin{cases} < \theta, \ \text{Decide } H_0 \\ \geq \theta, \ \text{Decide } H_1 \end{cases} \quad (16)$$

where

$$\begin{aligned} \Lambda_n(\mathbf{u}) &= \frac{P(\mathbf{u}|H_1)}{P(\mathbf{u}|H_0)} \\ &= \prod_{j=1}^{M} \frac{P\big(u_j|H_1\big)}{P\big(u_j|H_0\big)} \\ &= \prod_{\{K\}} \frac{P_{dj}(n)}{P_{fj}(n)} \cdot \prod_{\{M-K\}} \frac{1-P_{dj}(n)}{1-P_{fj}(n)} \end{aligned} \quad (17)$$

Here $\prod_{\{K\}}(\cdot)$ and $\prod_{\{M-K\}}(\cdot)$ mean to take into account all possible combinations of $\mathbf{u} = [u_1, u_2, \ldots, u_M]^{\mathrm{T}}$ meeting $n_1 = K$ and $n_0 = M - K$, where n_1 is the number of $u_j = 1$ and n_0 is the number of $u_j = 0$. It is worth noted that because the distance between each sensor and each network node is inconsistent, the correct detection probability and false alarm probability of each sensor are also different. The K-out-of-M rule we often used can be implemented by setting threshold, as follows

$$\begin{aligned} &\max\left(\prod_{\{K-1\}} \frac{P_{dj}(n)}{P_{fj}(n)} \cdot \prod_{\{M-K+1\}} \frac{1-P_{dj}(n)}{1-P_{fj}(n)}\right) < \theta \\ &\leq \min\left(\prod_{\{K\}} \frac{P_{dj}(n)}{P_{fj}(n)} \cdot \prod_{\{M-K\}} \frac{1-P_{dj}(n)}{1-P_{fj}(n)}\right). \end{aligned} \quad (18)$$

Let $K = M$ and $K = 1$ in (18), respectively, then we can get *AND* rule and *OR* rule as follows

AND rule:

$$\max\left(\prod_{\{M-1\}} \frac{P_{dj}(n)}{P_{fj}(n)} \cdot \prod_{\{1\}} \frac{1-P_{dj}(n)}{1-P_{fj}(n)}\right) < \theta$$

$$\leq \min\left(\prod_{\{M\}} \frac{P_{dj}(n)}{P_{fj}(n)}\right) \quad (19)$$

OR rule:

$$\max\left(\prod_{\{M\}} \frac{1-P_{dj}(n)}{1-P_{fj}(n)}\right) < \theta$$

$$\leq \min\left(\prod_{\{1\}} \frac{P_{dj}(n)}{P_{fj}(n)} \cdot \prod_{\{M-1\}} \frac{1-P_{dj}(n)}{1-P_{fj}(n)}\right) \quad (20)$$

To ensure that the above equation has a solution, the sufficient condition is $\max(P_{fj}(n)) \leq \min(P_{dj}(n))$. The correct detection probability and false alarm probability of FC are

$$\begin{aligned} \text{AND rule: } P_d(n) &= \prod_{j=1}^{M} P_{dj}(n) \\ P_f(n) &= \prod_{j=1}^{M} P_{fj}(n) \end{aligned} \quad (21)$$

$$\begin{aligned} \text{OR rule: } P_d(n) &= 1 - \prod_{j=1}^{M} \big(1 - P_{dj}(n)\big) \\ P_f(n) &= 1 - \prod_{j=1}^{M} \big(1 - P_{fj}(n)\big). \end{aligned} \quad (22)$$

More generally, for K-out-of-M rule, we have

$$\begin{aligned} P_d(n) &= \sum_{x=K}^{M} \binom{x}{M} \prod_{\{K\}} P_{dj}(n) \cdot \prod_{\{M-x\}} (1 - P_{dj}(n)) \\ P_f(n) &= \sum_{x=K}^{M} \binom{x}{M} \prod_{\{K\}} P_{fj}(n) \cdot \prod_{\{M-x\}} (1 - P_{fj}(n)). \end{aligned} \quad (23)$$

D. Soft Fusion of Influence Matrix

The above two methods both consider that the distributed sensors do not make topology inference, therefore, now we consider that not only FC but also distributed sensors can infer topology. The fusion method based on the fusion of the influence matrix is shown in Fig. 5(c). The distributed sensors carry out influence matrix by using Hawkes process, respectively, then report the results to the FC, which integrates the local influence matrix to get the final global influence matrix.

The topology inference without decision is a continuous variable between zero to one rather than a binary variable. In this case, the scheme considered in this section is a kind of soft fusion. Global topology inference at this point can be represented by the following equation

$$\mathbf{A} = \frac{1}{M} \sum_{j=1}^{M} \mathbf{A}^{(j)}, \quad (24)$$

where $\mathbf{A}^{(j)}$ is the local influence matrix of the *j*th sensor. This soft fusion is also equivalent to equal gain combination in spatial diversity.

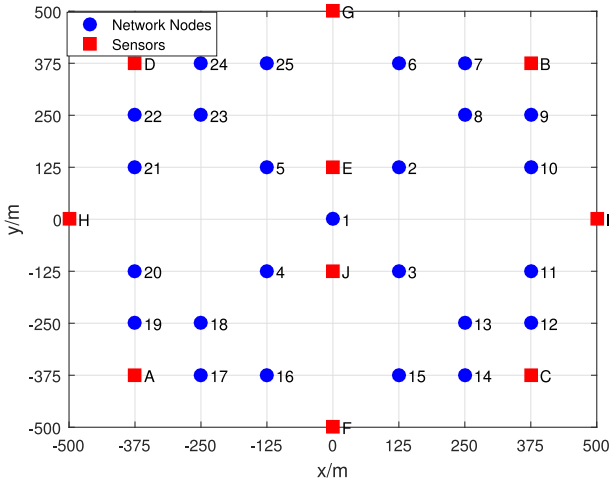

Fig. 6. Spatial distribution of target network nodes and sensors in simulations.

E. Hard Fusion of Influence Matrix

The fusion method to be considered in this section is also based on the fusion of the influence matrix, which is shown in Fig. 5(d). What is different from the scheme in Section III-D is that after the local topology inference, the distributed sensors will make topology decision. In this case, the distributed sensors report the binary influence matrix to the FC and then FC fuse the data to get global topology information.

The method in this section is a kind of hard fusion. The fusion criterion is the Neyman-Pearson criterion like the scheme based on the hard fusion of signal detections. Like Section II-B, the topology decision is also a binary hypothesis-testing problem

$$\begin{aligned} S_0 &: \text{ The two nodes are connected} \\ S_1 &: \text{ The two nodes are disconnected.} \end{aligned}$$

Moreover, the correct detection probability and false alarm probability of the jth sensor are given respectively by

$$\begin{aligned} P_{Dj} &= P(x=1|S_1) = P\big(A_{ij} \geq \alpha | S_1\big) \\ P_{Fj} &= P(x=1|S_0) = P\big(A_{ij} \geq \alpha | S_0\big) \end{aligned} \tag{25}$$

where α is the threshold of influence matrix and $x=1$ donates the decision that two nodes are connected. Correspondingly, $x=0$ donates the case that two nodes are disconnect. In this case, the LRT is given as follows:

$$\begin{aligned} \Lambda(\mathbf{x}) &= \frac{P(\mathbf{x}|S_1)}{P(\mathbf{x}|S_0)} \\ &= \prod_{j=1}^{M} \frac{P\big(x_j|S_1\big)}{P\big(x_j|S_0\big)} \\ &= \prod_{K} \frac{P_{Dj}}{P_{Fj}} \cdot \prod_{M-K} \frac{1-P_{Dj}}{1-P_{Fj}} \end{aligned} \tag{26}$$

The subsequent analysis of P_D and P_F is similar to that in Section III-C, which will not be repeated here.

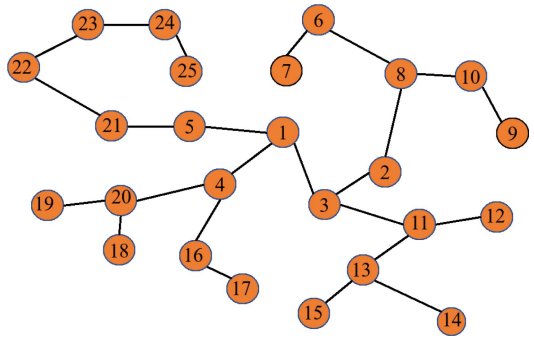

Fig. 7. Target wireless network topology in the simulations.

TABLE I
SIMULATION PARAMETERS

Parameter	Value
Number of nodes in networks N_{node}	25
Number of sensors M	1∼10
Communication protocol	ARQ
Sensing slot length	0.01 ms
Number of samples in each slot L	100
Event number N_{event}	10∼40
Number of sensing period Data length	2∼6 slot
ACK length	1 slot
Receiver noise spectral density n_0	-174dBm/Hz
Noise bandwidth W	10M
Signal transmit power P_s	-15dBmW∼-5dBmW
Signal detection threshold ζ	4×10^{-14}W
Influence matrix threshold α	0.03

IV. SIMULATION AND DISCUSSIONS

A. Simulation Setup

In this section, we provide computer simulations to demonstrate the effectiveness of the proposed cooperative topology sensing schemes and discuss the impact of various parameter configurations. Without loss of generality, in the following simulations, we consider a relative complex target wireless network with its node distribution and topology connectivity shown in Fig. 6 and Fig. 7, respectively. 25 nodes in the target wireless network and 10 sensors in the sensor network are located in a 1 km $\times$ 1 km area, in which the locations of 25 nodes are fixed and the locations of 10 sensors are uniform random distribution. The network has a distributed topology shown in Fig. 7. Other simulation parameters are set in Tab. I. The following two metrics are utilized to evaluate the performance of scheme, which are as follows.

1) Structural Hamming Distance (SHD): It measures the minimum number of edge additions, and/or removals necessary to convert an estimated graph into the true graph, which can be given by

$$SHD = E - TP + FP \tag{27}$$

where E is the total number of links in the actual network, TP denotes the number of true positives, and FP is the number of false positives [43].

2) Receiver Operating Characteristic (ROC) Curve: We also use ROC curve to compare performance of the different parameters, where $TPR = \frac{TP}{E}$ quantifies the true positive rate, FNR =1–TPR is the false negative rate and FPR =

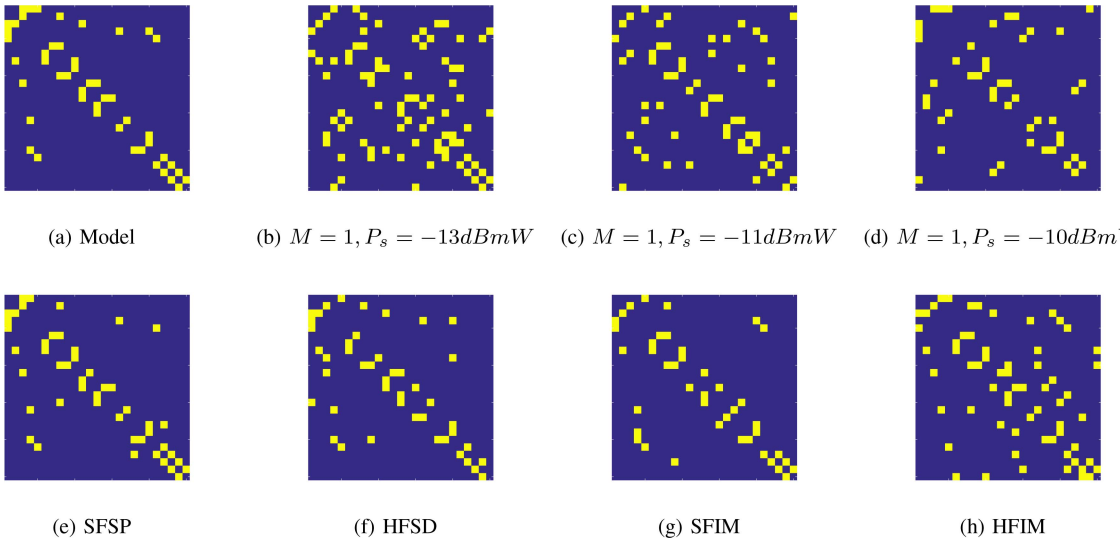

(a) Model (b) $M = 1, P_s = -13dBmW$ (c) $M = 1, P_s = -11dBmW$ (d) $M = 1, P_s = -10dBmW$

(e) SFSP (f) HFSD (g) SFIM (h) HFIM

Fig. 8. Some examples of influence matrix, in which the yellow represents that the two nodes are connected and the blue represents that the two nodes are disconnected. The subfigure (a) is the true influence matrix and the subfigures (b) (c) (d) are the results with single sensor under different P_s, in which $N_{event} = 10$. The subfigures (e) (f) (g) (h) are the results with multi-sensor under different schemes, in which $M = 5$, $N_{event} = 10$ and $P_s = -13$ dBmW.

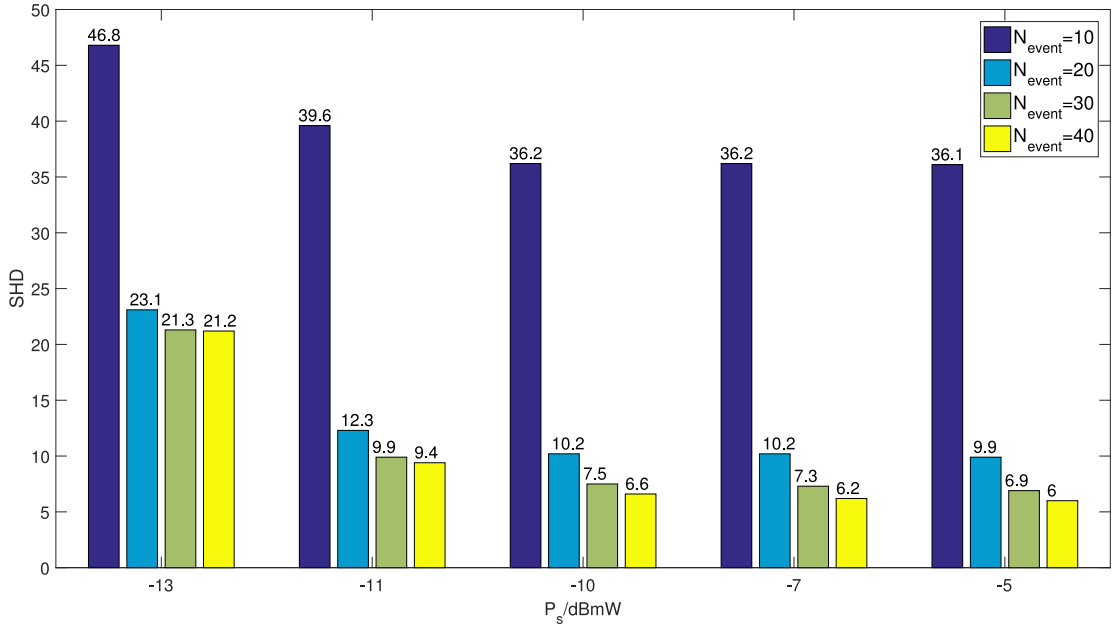

Fig. 9. The SHD performance of topology sensing with single sensor under various parameters.

$\frac{FP}{N(N-1)-E}$ quantifies the false positive rate [44]–[46]. The ROC curves as follows are the average of multiple Monte Carlo simulations.

B. Results of Topology Sensing With Single Sensor

Some influence matrixes recovered with single sensor are shown in the first line of Fig. 8, in which we can see the results visually. Here we use SHD to evaluate the performance of topology sensing scheme with single sensor, which is shown in Fig. 9. The lower the SHD is, the better the sensing performance will be. The simulation results are the average of 100 topology sensing processes, that is why some of SHDs are discrete. Given the value of transmit power, the performance has a trend of improving with the increase of the event number, especially when it changes from $N_{event} = 10$ to $N_{event} = 20$. It is because that event number is too less to support subsequent topology sensing algorithm.

On the other hand, given the value of event number, [1]the performance has a trend of improving with the increase of the transmit power. However, it cannot be ignored that the performance in $P_s = -13$ dBmW to $P_s = -10$ dBmW is improving but in $P_s = -7$ dBmW to $P_s = -5$ dBmW is almost identical. The above phenomenon indicates that there is

[1]Event number means the average used times of each link. For example, if there are 48 links in the network and $N_{event} = 10$, the effective sample number is 480. However, because of the unreliable information from signal detection, the false alarm probability p_f and missed detection probability p_m are present. Thus, the actual number of samples cannot be given accurately.

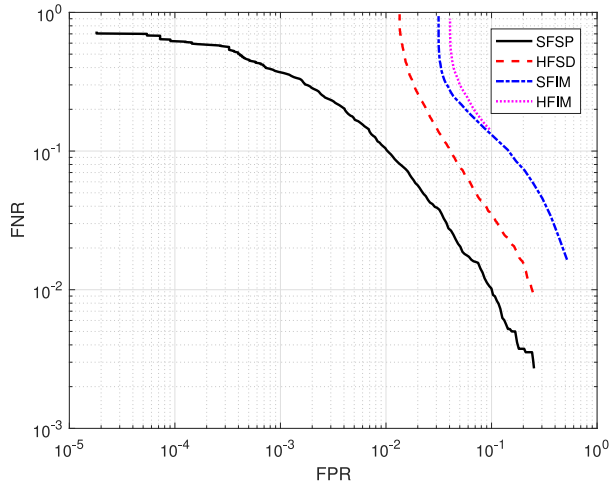

(a) ROC curve of four fusion methods.

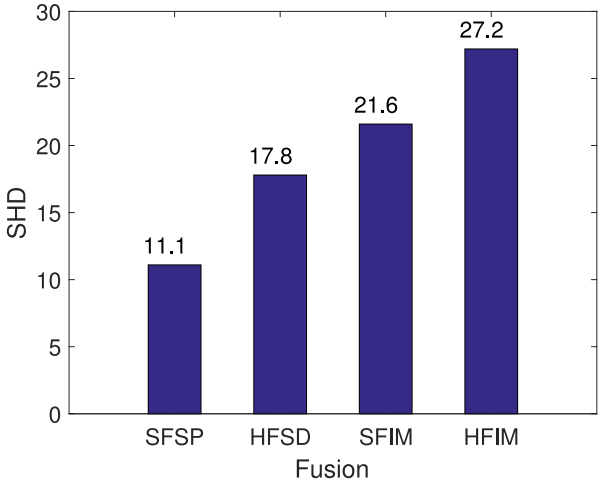

(b) SHDs of four fusion methods.

Fig. 10. The comparison of four fusion methods.

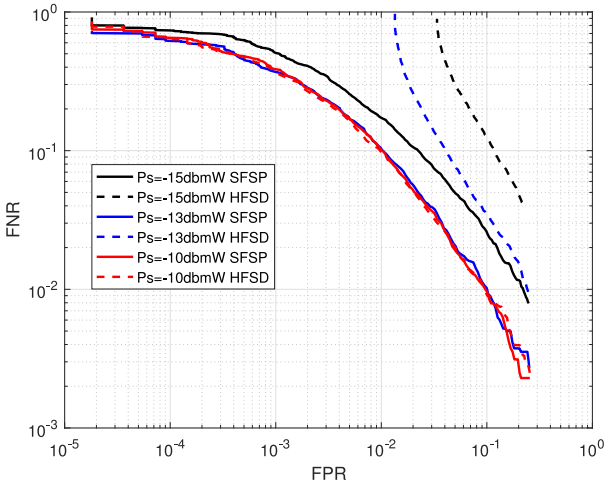

Fig. 11. The impact of transmit power P_s in the case of SFSP and HFSD, respectively.

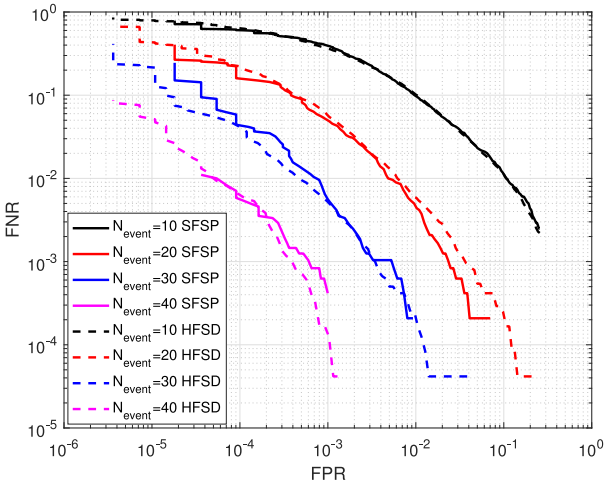

Fig. 12. The impact of event number N_{event} in the case of SFSP and HFSD, respectively.

a limit of sensing accuracy when the transmit power is higher enough, which is power saturated. Moreover, the phenomenon of power saturated will be more obvious when event number is less.

C. Results of Cooperative Topology Sensing

In this section, the cooperative topology sensing scheme based on four fusion methods are simulated, respectively. Some influence matrixes recovered with multi-sensor are shown in the second line of Fig. 8, in which we can see the results visually. ROC curve is used to evaluate the performance of cooperative topology sensing scheme with multi-sensor and the sensing accuracies with different parameters are analyzed as follows. The comparison of four fusion methods is shown in Fig. 10. Except for the parameters already determined in Tab. I, the uncertain parameters are set as follows, the number of sensors is $M = 5$, transmit power $P_s = -13$ dBmW, event number $N_{event} = 10$ and the rule is K-out-of-M rule.

Fig. 10(a) is the ROC curve of four fusion methods, in which we can found that among the four fusion methods, the performance of SFSP is the best and the performance of HFIM is the worst. It is because that when every time distributed sensors make a decision, a part of information will be lost. The more original the data reported by distributed sensors to the FC is, the better the performance will be. In order to elucidate problem more intuitively, the SHDs of four fusion methods are shown in Fig. 10(b), in which the same result will be found.

1) The Impact of Transmit Power P_s: The impact of transmit power P_s in four fusion methods is almost the same, so we will analyze the SFSP and HFSD as examples in this section.

Fig. 11 shows the ROC curve in the cases of different transmit power P_s, in which the number of sensors is $M = 5$ and the event number is $N_{event} = 10$. All the solid lines denote the performance in the case of SFSP and all the dotted lines denote the performance in the case of HFSD. It is observed that the performance improves with the increase of P_s and the power saturated phenomenon is also observable when compares the cases $P_s = -10$ dBmW and $P_s = -13$ dBmW. What is different from the single sensor sensing is that the value of saturated power is lower for multi-sensor cooperative

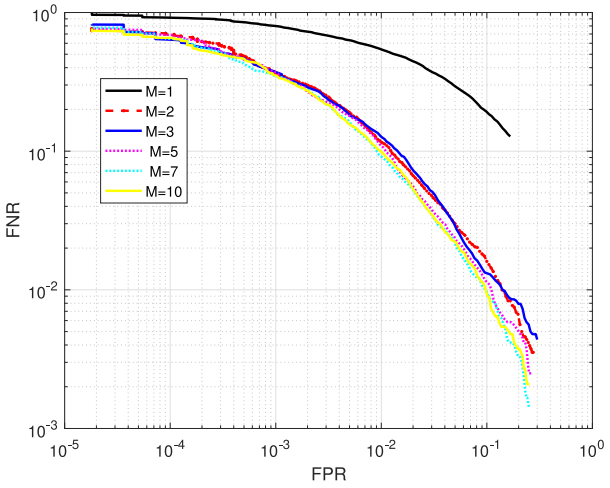

(a) The impact of M in the case of SFSP.

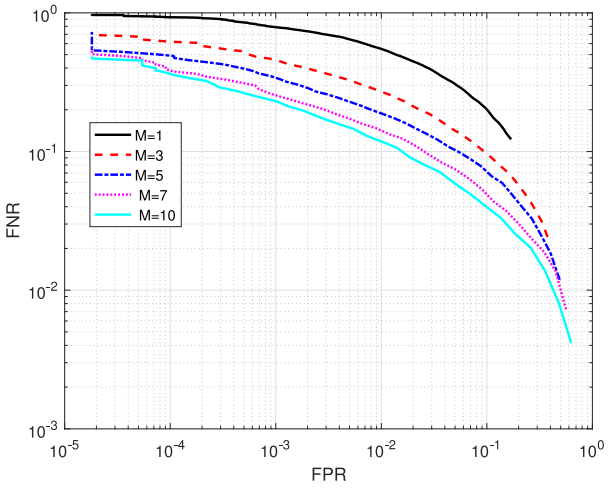

(b) The impact of M in the case of SFIM.

Fig. 13. The impact of the number of sensors *M* in the case of SFSP and SFIM, respectively.

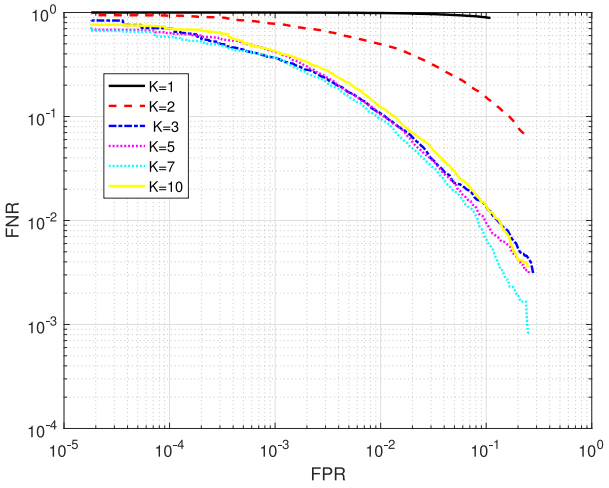

(a) The impact of K in the case of HFSD.

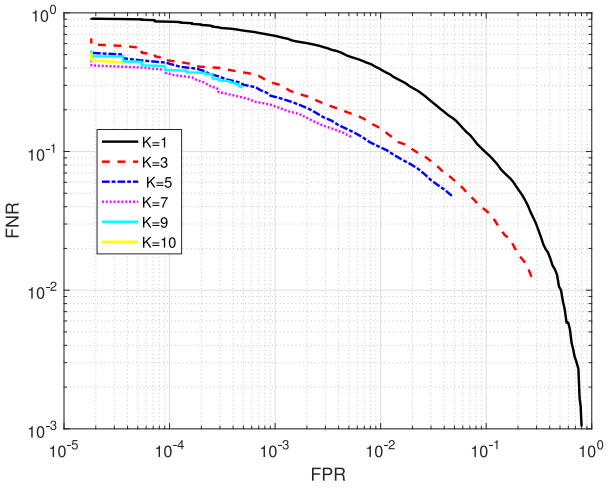

(b) The impact of K in the case of HFIM.

Fig. 14. The impact of the *K* in the *K*-out-of-*M* Rule in the case of HFSD and HFIM, respectively.

sensing, which suggests that the sensitivity of multi-sensor is improved. Then, comparing two lines of the same color, there are two results found: First, in the case of unsaturation, the performance of SFSP is better than that of HFSD. Second, in the case of saturation, two method have the same limit performance but the value of saturated power in SFSP is lower than that in HFSD. Moreover, there is a lower boundary of *FPR*, which is obvious with the low P_s. It is because that the lower boundary of P_f, see [47] for detail.

2) The Impact of Event Number N_{event}: The impact of event number N_{event} in four fusion methods is almost the same, so we will analyze the SFSP and HFSD as examples in this section, too.

The impact of event number is shown in Fig. 12, in which the number of sensors is $M = 5$ and the transmit power is $P_s = -10$ dBmW. Here the reason why we set a high transmit power is to eliminate its interference to the simulations. All the solid lines denote the performance in the case of SFSP and all the dotted lines denote the performance in the case of HFSD. It is obvious that the more the event number is, the

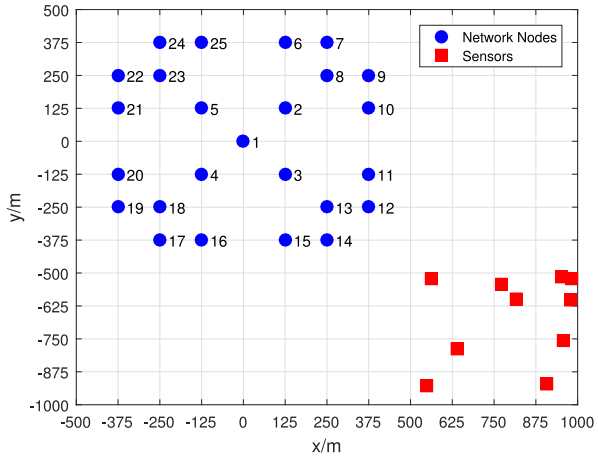

Fig. 15. Spatial distribution of target network nodes and clustered sensors.

better the performance will be. This further validates that the effect of statistical learning depends largely on the amount of data. Moreover, comparing two lines of the same color, it is

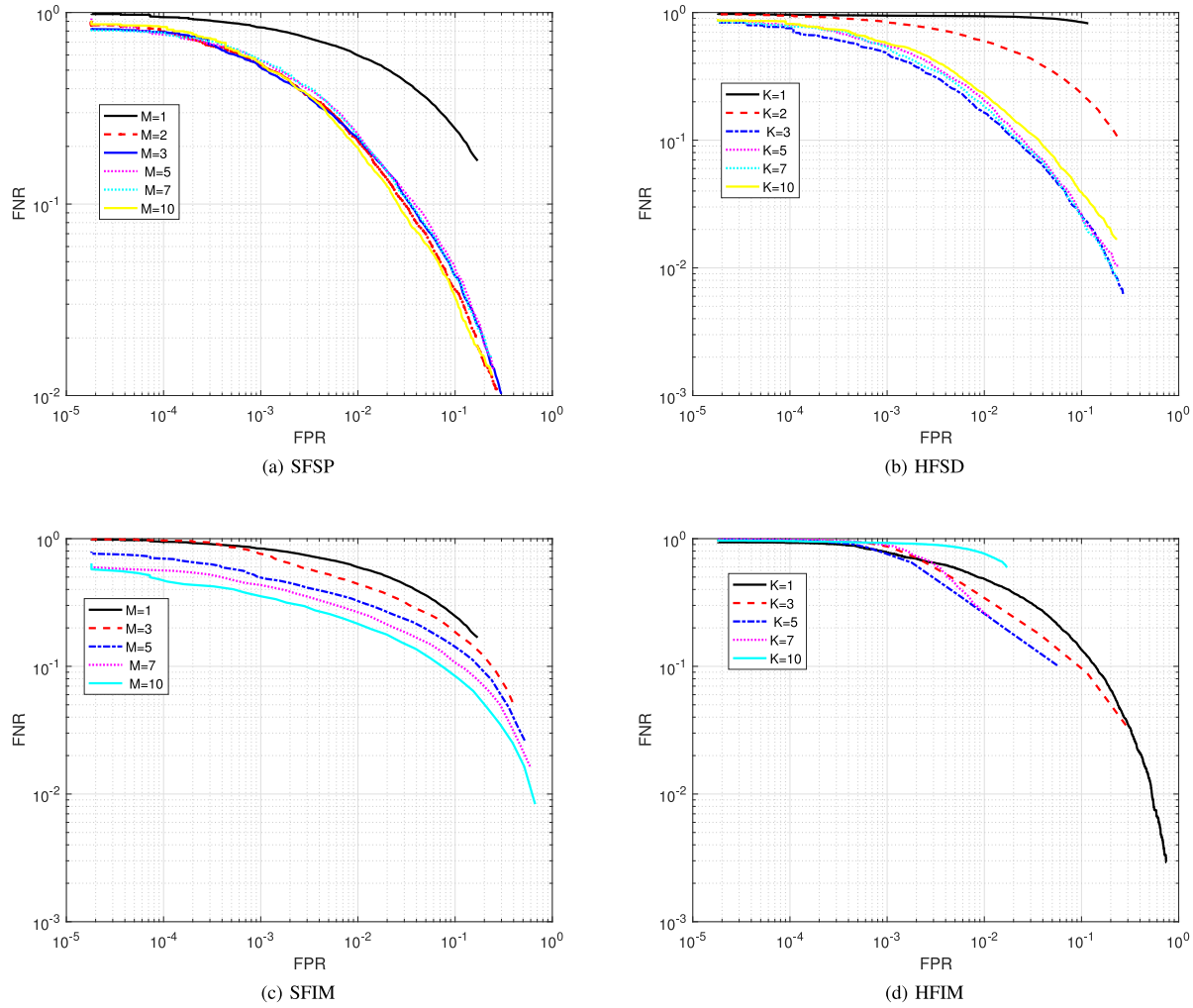

(a) SFSP (b) HFSD

(c) SFIM (d) HFIM

Fig. 16. The results in the case of clustered sensors.

found that the performance of two methods is almost the same under the different value of event number in the case of power saturation.

3) The Impact of the Number of Sensors M: The impact of the number of sensors M is shown in Fig. 13, in which the transmit power is $P_s = -10$ dBmW and the event number is $N_{event} = 10$.

It is believable that the more sensors there are, the better the system will perform, however, the result shown in Fig. 13(a) is different from our intuition. Fig. 13(a) shows the impact of the number of sensors M in the case of SFSP and the trend of HFSD is almost the same with SFSP. It can be found that the performance with multi-sensor is better than that with single senor, however, the sensing accuracy is not improved with the increase of M. The performance of $M = 3, 5, 7, 10$ is almost the same, which can be explained by sensor location and fusion rule. The density of sensor settings makes it difficult to increase much useful information by increasing the number of sensors, and the use of K-out-of-M rule also contributed to the loss of information.

Fig. 13(b) shows the impact of the number of sensors M in the case of SFIM and the trend of HFIM is almost the same with SFIM. It is observed that, unlike Fig. 13(a), the large number of sensors perform better than a few sensors. It is because that for influence matrix, the more sensors mean more data.

Comparing Fig. 13(a) and Fig. 13(b), it suggests that the fusion of signal detection data is insensitive to M, but the fusion of the influence matrix is sensitive to M, whether soft fusion or hard fusion.

4) The Impact of the K in the K-out-of-M Rule: Fig. 14 shows the performance with different K in the K-out-of-M rule, where the transmit power is $P_s = -10$ dBmW, the event number is $N_{event} = 10$ and the number of sensors is $M = 10$.

Fig. 14(a) shows the impact of K in the case of HFSD. It is found that the performance is improved a lot when the value of K changes from 1 to 3 but the performance is almost the same when $K = 3, 5, 7, 10$. It is because that in the simulation initialization, we assume that the noise is random. Therefore, the signal is easily detected by more than two sensors but the noise is difficult to be detected by more than two sensors at the same time. These result in the improvement of performance with $K = 1, 2, 3$.

Fig. 14(b) shows the impact of K in the case of HFIM. It is found that the performance in $K = 1$ is the worst and the performance in $K = 7$ is the best. As the K increases,

TABLE II
OVERHEAD OF FOUR FUSION METHODS

	SFSP	HFSD	SFIM	HFIM
Overhead(o)	$(p+q)n_{data}M$	$(p+r)n_{data}M$	oN_{node}^2M	N_{node}^2M
Normalized Overhead	1	$\frac{q+r}{p+q}$	$\frac{oN_{\text{node}}}{(p+q)n_{\text{data}}}$	$\frac{N_{\text{node}}}{(p+q)n_{\text{data}}}$

TABLE III
THE UNIT OVERHEAD EFFICIENCY OF FOUR FUSION METHODS

	SFSP	HFSD	SFIM	HFIM
Unit Overhead Efficiency	0.9815	1.2725	12.3392	122.1973

performance tends to get better first and then get worse, which is different from the results in Fig. 14(a). It because that when the value of *K* is relatively small, there may be lots of redundant links discovered and when the value of *K* is relatively large, there may be lots of true links missed. At the same time, it is observed that the ROC curve is becoming shorter with the *K* increases. Due to the amount of unfused data is the same, a larger value of *K* means less data available.

5) The Impact of Sensors' Locations: The simulation setup in Fig. 6 assumes that the target network and sensors are scattered in the same area, but in some cases, the sensors may not be close enough to the target network. Thus, it is necessary to consider the impact of sensors' locations in this section. Instead of dispersed sensors, the case that the sensors are clustered outside the target network is simulated. The locations of network nodes and sensors are shown in Fig. 15, in which the sensors are placed randomly in the 500 *m* $\times$ 500 *m* rectangular area centered (750, -750). The results are shown in Fig. 16 and prove that the cooperative topology sensing schemes we proposed show good performance in the case of not only dispersed sensors but also clustered sensors. Comparing Fig. 16 with Fig. 13 and Fig. 14, it can be found that the trend shown by the four schemes is basically the same. Specifically, as the number of sensors *M* increases, the performance of SFSP remain unchanged and the performance of SFIM gets better. As the *K* increase, the performance of HFSD improves with $K = 1, 2, 3$ and the performance of HFIM gets better first and then worse. Actually, the results in Fig. 13 and Fig. 14 are a little better than that in Fig. 16. It can be explained by distance between the sensors and nodes, but it cannot say that the setup of dispersed sensors is better than that of clustered sensors.

D. The Comparison of the Four Fusion Methods

As shown in Fig. 10, sorting the four fusion methods by performance from good to bad is SFSP, HFSD, SFIM, HFIM. However, the more original the data reported is, the larder the amount of data will be, which causes resource occupation. Therefore, sorting the four fusion methods by resource occupation from less to more is HFIM, SFIM, HFSD, SFSP. Actually, it is necessary to balance the contradiction of resource occupancy and sensing accuracy in practice. When using SFSP, the sensors must report mass data to FC, which will correspond to more reporting overhead. When using HFIM, FC only receives local decision so that information loss is present.

The way to balance the overhead and the performance is as follows. First, let us define a statistic

$$B = f(o, e),$$

in which *o* is the overhead and *e* is the efficiency or the accuracy. The overhead mainly occurs in the process of reporting data from distributed sensors to fusion center. Supposing that the average cost of transmitting a packet per communication link is *c* , the overhead of transferring n_0 packets is obtained by $o = n_0 c$. n_0 can be calculated by $n_0 = \frac{n_{\text{data}}}{n_s}$ in which n_{data} is the number of reported data (the data may be signal power, the time series, soft adjacency matrix or hard adjacency matrix) and n_s is the number of data transmitted per packet. Further, the normalized overhead can be obtained by $o_n = \frac{n_0 c}{n_{0,\max} c} = \frac{n_0}{n_{0,\max}}$, in which $n_{0,max}$ is the maximum number of packets. Then, we can calculate the efficiency with $e = 1 - \frac{SHD}{(N_{\text{node}}-1)N_{\text{node}}}$.

Actually, the choice of *f* function is task driven, which determines the priority of overhead and efficiency. For, example, we make it as

$$B = \frac{e}{o_n} = \frac{SHD \cdot n_{0,\max}}{(N_{\text{node}} - 1)N_{\text{node}} \cdot n_0},$$

by using which to simply show the relationship between the overhead and the efficiency. We can call it unit overhead efficiency.

The overhead of four fusion methods are shown in the Table II, in which *p, q, s* denote *p* bits quantization of event sequence, *q* bits quantization of soft signal detection data, and *s* bits quantization of soft adjacency matrix, respectively. *r* is the percentage of binary signal detection data in soft signal detection data such that $r \in [0, 1]$. It is observed that $o_{n,SFSP} > o_{n,\text{HFSD}} \gg o_{n,SFIM} > o_{n,HFIM}$. In order to make this problem more intuitive, combining the results of Fig. 10(b), the unit overhead efficiency of four fusion method is shown in Table III with $n_{data} = 5000$, $p = 4$, $q = 12$, $s = 10$, $r = 0.2$. The other parameters are $P_s = -13$ dBmW, $N_{event} = 10$, $M = 5$. From this perspective, HFIM is the most recommended cooperative topology sensing scheme.

E. The Scalability of Cooperative Topology Sensing Schemes

With the development of large-scale networks, the scalability of system has become an important part to evaluate scheme. The scalability of a system refers to its ability to adapt changes, which can be explained by runtime and performance.

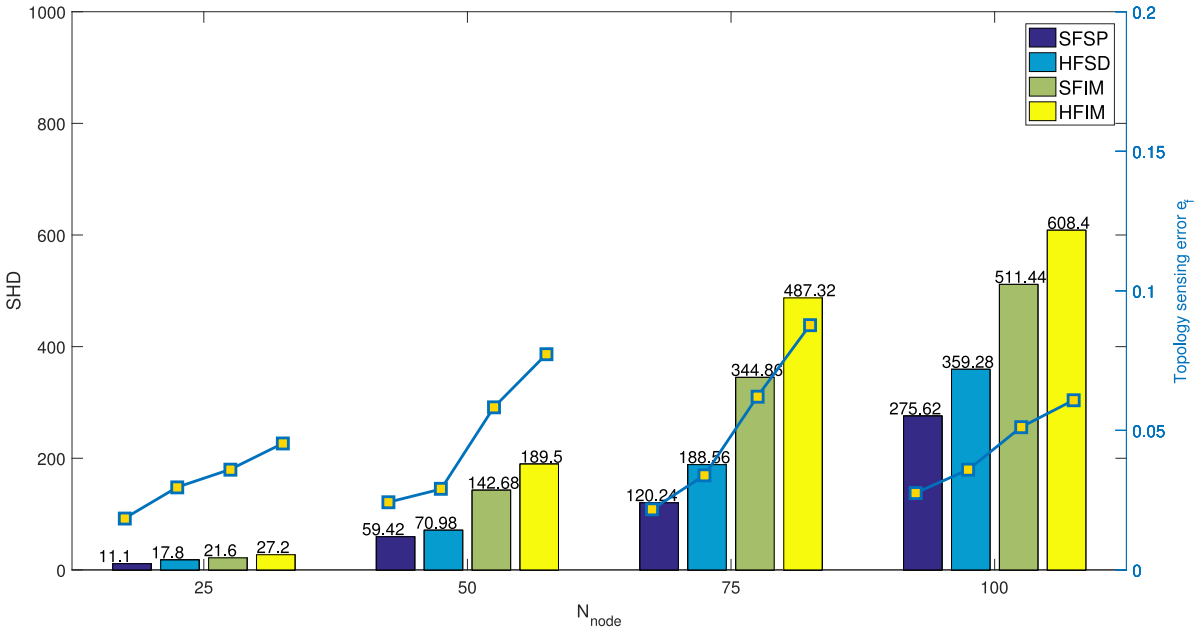

Fig. 17. The results in the case of different number of network nodes.

First, from the perspective of runtime, the convergence rate and computational complexity of the algorithm is what we care about. Beside the data fusion, the core of this problem is to solve a maximum likelihood function and we elaborate its solving process in Appendix A. Taking Newton's method as example, it is noted for fast convergence rate. As for its computational complexity, there is not a clear derivation but it can be known in the $[c_L(\lg t - \lg\lg t), c_U \lg(1+t)]$, where $t = max(1, \lg 1/\epsilon)$ [48]. Because of the inverse of Hessian matrix, the complexity is increasing with N_{node}^2, which can be accepted when there are a large number of nodes in the network. Actually, taking the inverse of Hessian matrix can be avoided by Quasi-newton method or conjugate gradient method.

Then, from the perspective of performance, we consider a new case of adding the number of network nodes. We randomly placed the target network with 25, 50, 75 and 100 nodes in an 1 $km \times 1km$ area, respectively. Then, we also randomly placed 5 distributed sensors in the same area. The results are shown in the Fig. 17, in which the bars show the SHD of four schemes under different number of nodes and the lines show the corresponding sensing error rate $e_f = \frac{SHD}{(N_{\text{node}}-1)N_{\text{node}}}$. It is observed that as the number of nodes increases, the performance of the methods we proposed does not decrease gradually.

Therefore, it is reasonable to say that the schemes we proposed is scalable from the perspective of whether runtime and performance.

F. The Performance in the Presence of RF Transmitter Recognition Errors

The signal detection errors have been considered, modeled and simulated in the above sections, but in the realistic scenario, RF transmitter recognition errors are often present

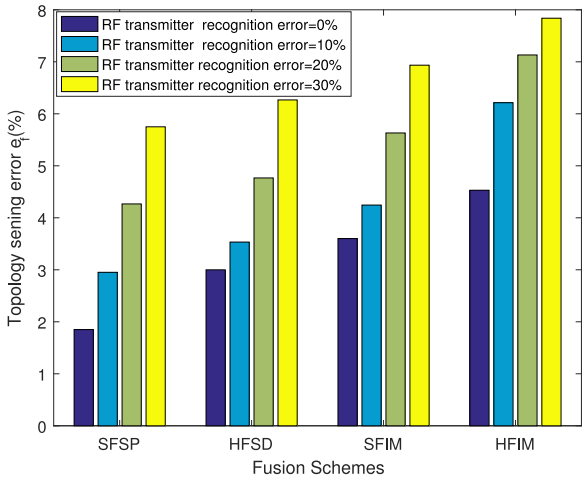

Fig. 18. The topology sensing error rate of four fusion methods in the case of RF transmitter recognition error.

besides signal detection errors. If the list of nodes is known in advance, the identification of sender or the RF transmitter recognition is generally modeled as a close set classification problem as discussed in [49]–[51]. By comparing the received signal features with the known node features, the sender of the signal can be identified. These features may be RF fingerprint [49], signal parameter characteristic [52], [53] and so on. However, if the list of nodes is unavailable, the identification of sender or the RF transmitter recognition can be modeled as an open set identification problem as discussed in [27], [54]. This kind of approaches can be used to identify the source device without a particular target device to compare it against.

It should be noted that the RF transmitter recognition errors may be present whether an open set recognition method is used or a closed set recognition method is used. In order to

explore the impact of the RF transmitter recognition errors, we consider that the RF transmitter recognition is not always right but with random errors and the probability of identification as other each node is the same. The topology sensing errors of four fusion schemes in the case of 0%,10%,20%,30% RF transmitter recognition errors are shown and compared in Fig. 18. No doubt that the performance of schemes gets worse with the RF transmitter recognition error increasing. However, even in the case of 30% RF transmitter recognition error, the schemes can still maintain accuracy above 90%. It is observed that the schemes we proposed are robust to some extent for the RF transmitter recognition error. It also further demonstrates the superiority of the collaborative topology sensing framework to deal with limited and unreliable information.

V. Conclusion and Future Work

In this article, we investigate the issue of cooperative topology sensing using limited and unreliable information. Firstly, we develop a cooperative topology sensing framework to exploit multi-sensor spatial diversity for coping with wireless randomness. Then, based on the observation that in wireless networks, we formulate the communication events among multiple wireless transceivers as multi-dimensional Hawkes process. Further, we propose and analyze four cooperative topology sensing schemes with multiple distributed sensors from the perspective of hard fusion and soft fusion, respectively. In addition, we use structural hamming distance and receiver operating characteristic curve to evaluate the performance of single sensor topology sensing and cooperative topology sensing. The simulation results show that the signal transmit power and event number have great influence on sensing accuracy and cooperative topology sensing is an effective measure to deal with the issues of wireless channel randomness.

The research of topology sensing of wireless networks is a fruitful area but still in the preliminary stage. Further research will be conducted to investigate several issues as follows:

1) Heterogeneous Data Fusion: With the popularization of large-scale network, it is generally impractical for every sensor to perceive the whole network, due to the limited coverage of wireless networks and the limited sensitivity of sensors. The requirements of topology sensing will also develop from local topology to global topology.

2) Joint Optimization of Multiple Thresholds: There are multiple thresholds in the data fusion scheme mentioned in this article, such as the signal detection, influence matrix, and Neyman-Pearson criterion, etc. How to combine these thresholds to achieve optimal performance is a huge challenge for topology sensing scheme.

3) Online Network Topology Sensing: In complex network scenarios, the nodes may have mobility such that the topology changes over time. At this point, the offline topology sensing algorithm will no longer be applicable because of its timeliness. Investigating the issue about online network topology sensing and tracking method is a significant research.

Appendix A
Solving Process of Maximum Likelihood Function

The objective function is

$$[\mu, \mathbf{A}] = \underset{\mu,\mathbf{A}}{\operatorname{argmin}} \mathcal{L}(\mu, \mathbf{A}) = \sum_i \mathcal{L}_i(\mu, A). \tag{28}$$

There are $N(N+1)$ parameters in the above equation, which is difficult to optimization directly. Since each likelihood depends on only an isolated subset of the parameters, each term can be optimized individually. Substituting the equation (8) into equation (9) we can get

$$\begin{aligned} L_i(\mu, A) &= \int_0^T \lambda_i(n)dn - \sum_{k_i \in K_i} \log \lambda_i\left(n_{k_i}\right) \\ &= \int_0^T \left[\mu_i + \sum_j A_{ij} \sum_{k_j \in K_j} \gamma\left(n - n_{k_j}\right)\right] dn \\ &\quad - \sum_{k_i \in K_i} \log \left[\mu_i + \sum_j A_{ij} \sum_{k_j \in K_j} \gamma\left(n_{k_i} - n_{k_j}\right)\right] \\ &= \mu_i T + \sum_j A_{ij} \sum_{k_j \in K_j} \int_0^T \gamma\left(n - n_{k_j}\right) dn \\ &\quad - \sum_{k_i \in K_i} \log \left[1 \cdot \mu_i + \sum_j A_{ij} \sum_{k_j \in K_j} \gamma\left(n_{k_i} - n_{k_j}\right)\right] \end{aligned} \tag{29}$$

To simplify the presentation, we define $R_j = \sum_{k_j \in K_j} \int_0^N \gamma(n - n_{k_j})dn$, $r_{ij} = \sum_{k_j \in K_j} \gamma(n_{k_i} - n_{k_j})$. Then, the above equation can be converted into

$$\begin{aligned} &L_i(\mu, A) \\ &= \mu_i N + \sum_j A_{ij} R_j - \sum_{k_i \in K_i} \log \left(1 \cdot \mu_i + \sum_j A_{ij} r_{ij}\right) \\ &= \begin{bmatrix} N & R_1 & R_2 & \cdots & R_{N_{\text{node}}} \end{bmatrix} \begin{bmatrix} \mu_i \\ A_{i1} \\ A_{i2} \\ \vdots \\ A_{iN_{\text{node}}} \end{bmatrix} \\ &\quad - \sum_{k_i \in K_i} \log \begin{bmatrix} 1 & r_{i1} & r_{i2} & \cdots & r_{iN_{node}} \end{bmatrix} \begin{bmatrix} \mu_i \\ A_{i1} \\ A_{i2} \\ \vdots \\ A_{iN_{node}} \end{bmatrix} \end{aligned} \tag{30}$$

If we define $R_0 = T, A_{i0} = \mu_i, r_{i0} = 1$, the above equation can be written in matrix form as

$$L_i(\mathbf{A}) = \mathbf{RA} - \mathbf{1}' \cdot \log \mathbf{rA}.$$

The above equation is a convex function since the second derivative is non-negative. Thus, there are many ways to solve the above equation, which are not repeated here. In the simulation, we choose the Newton's method because of its rate of convergence [15].

REFERENCES

[1] D. Easley and J. Kleinberg, "Networks, crowds and markets: Reasoning about a highly connected world," *J. Roy. Stat. Soc.*, vol. 175, no. 4, p. 1073, 2012.

[2] C. Goodwin, "Action and embodiment within situated human interaction," *J. Pragmat.*, vol. 32, no. 10, pp. 1489–1522, 2000.

[3] M. Rubinov and O. Sporns, "Complex network measures of brain connectivity: Uses and interpretations," *Neuroimage*, vol. 52, no. 3, pp. 1059–1069, 2010.

[4] D. Zhang and L. Zhou, "Discovering golden nuggets: Data mining in financial application," *IEEE Trans. Syst., Man, Cybern. C, Appl. Rev.*, vol. 34, no. 4, pp. 513–522, Nov. 2004.

[5] Z. Zhang, Y. Hung, S. Chan, W. Xu, and Y. Hu, "Modeling and identification of gene regulatory networks: A granger causality approach," in *Proc. Int. Conf. Mach. Learn. Cybern.*, Qingdao, China, 2010, pp. 3073–3078.

[6] E. Kolaczyk, *Statistical Analysis of Network Data*. New York, NY, USA: Springer, 2009.

[7] S. Segarra, A. Marques, G. Mateos, and A. Ribeiro, "Network topology inference from spectral templates," *IEEE Trans. Signal Inf. Process. Netw.*, vol. 3, no. 3, pp. 467–483, Sep. 2017.

[8] G. Mansfield, M. Ouchi, K. Jayanthi, Y. Kimura, K. Ohta, and Y. Nemoto, "Techniques for automated network map generation using SNMP," in *Proc. INFOCOM IEEE 15th Joint Conf. Comput. Soc. Netw. Next Gener.*, San Francisco, CA, USA, 1996, pp. 473–480.

[9] A. Shaikh, M. Goyal, A. Greenberg, R. Rajan, and K. Ramakrishnan, "An OSPF topology server: Design and evaluation," *IEEE J. Sel. Areas Commun.*, vol. 20, no. 4, pp. 746–755, May 2002.

[10] G. Giannakis, Y. Shen, and G. Karanikolas, "Topology identification and learning over graphs: Accounting for nonlinearities and dynamics," *Proc. IEEE*, vol. 106, no. 5, pp. 787–807, May 2018.

[11] K. Friston, L. Harrison, and W. Penny, "Dynamic causal modelling," *Neuroimage*, vol. 19, no. 4, pp. 1273–1302, 2003.

[12] P. Tilghman and D. Rosenbluth, "Inferring wireless communications links and network topology from externals using granger causality," in *Proc. Military Commun. Conf.*, San Diego, CA, USA, 2014, pp. 1284–1289.

[13] M. Laghate and D. Cabric, "Learning wireless networks' topologies using asymmetric granger causality," *IEEE J. Sel. Topics Signal Process.*, vol. 12, no. 1, pp. 233–247, Feb. 2018.

[14] M. Moore and M. Davenport, "Analysis of wireless networks using hawkes processes," in *Proc. IEEE 17th Int. Workshop Signal Process. Adv. Wireless Commun.*, Edinburgh, U.K., 2016, pp. 1–5.

[15] M. Moore and M. Davenport, "A hawkes' eye view of network information flow," in *Proc. IEEE Stat. Signal Process. Workshop*, Palma de Mallorca, Spain, 2016, pp. 1–5.

[16] P. Sharma, D. Bucci, S. Brahma, and P. Varshney, "Communication network topology inference via transfer entropy," *IEEE Trans. Netw. Sci. Eng.*, vol. 7, no. 1, pp. 562–575, Jan.–Mar. 2020.

[17] X. Dong, D. Thanou, M. Rabbat, and P. Frossard, "Learning graphs from data: A signal representation perspective," *IEEE Signal Process. Mag.*, vol. 36, no. 3, pp. 44–63, May 2019.

[18] G. Mateos, S. Segarra, A. G. Marques, and A. Ribeiro, "Connecting the dots: Identifying network structure via graph signal processing," *IEEE Signal Process. Mag.*, vol. 36, no. 3, pp. 16–43, May 2019.

[19] S. Sardellitti, S. Barbarossa, and P. Lorenzo, "Graph topology inference based on sparsifying transform learning," *IEEE Trans. Signal Process.*, vol. 67, no. 7, pp. 1712–1727, Apr. 2019.

[20] Y. Shen, X. Fu, G. B. Giannakis, and N. D. Sidiropoulos, "Topology identification of directed graphs via joint diagonalization of correlation matrices," *IEEE Trans. Signal Inf. Process. Netw.*, vol. 6, pp. 271–283, 2020, doi: 10.1109/TSIPN.2020.2984131.

[21] A. Sendonaris, E. Erkip, and B. Aazhang, "User cooperation diversity. Part I. System description," *IEEE Trans. Commun.*, vol. 51, no. 11, pp. 1927–1938, Nov. 2003.

[22] A. Sendonaris, E. Erkip, and B. Aazhang, "User cooperation diversity. Part II. Implementation aspects and performance analysis," *IEEE Trans. Commun.*, vol. 51, no. 11, pp. 1939–1948, Nov. 2003.

[23] Q. Wu *et al.*, "Cognitive Internet of Things: A new paradigm beyond connection," *IEEE Internet Things J.*, vol. 1, no. 2, pp. 129–143, Apr. 2014.

[24] Q. Wu, G. Ding, J. Wang, and Y. Yao, "Spatial-temporal opportunity detection for spectrum-heterogeneous cognitive radio networks: Two-dimensional sensing," *IEEE Trans. Wireless Commun.*, vol. 12, no. 2, pp. 516–526, Feb. 2013.

[25] H. Stanislaw and N. Todorov, "Calculation of signal detection theory measures," *Behav. Res. Methods Instrum. Comput.*, vol. 31, no. 1, pp. 137–149, 1999.

[26] G. Mao, B. Fidan, and B. Anderson, "Wireless sensor network localization techniques," *Comput. Netw.*, vol. 51, no. 10, pp. 2529–2553, 2007.

[27] K. Merchant, S. Revay, G. Stantchev, and B. Nousain, "Deep learning for RF device fingerprinting in cognitive communication networks," *IEEE J. Sel. Topics Signal Process.*, vol. 12, no. 1, pp. 160–167, Feb. 2018.

[28] S. Zheng *et al.*, "Big data processing architecture for radio signals empowered by deep learning: Concept, experiment, applications and challenges," *IEEE Access*, vol. 6, pp. 55907–55922, 2018.

[29] S. Chen, S. Zheng, L. Yang, and X. Yang, "Deep learning for large-scale real-world ACARS and ADS-B radio signal classification," *IEEE Access*, vol. 7, pp. 89256–89264, 2019.

[30] J. Ma and G. Li, "Soft combination and detection for cooperative spectrum sensing in cognitive radio networks," *IEEE Trans. Wireless Commun.*, vol. 7, no. 11, pp. 4502–4507, Nov. 2008.

[31] S. Herath, N. Rajatheva, and C. Tellambura, "On the energy detection of unknown deterministic signal over nakagami channelswith selection combining," in *Proc. Can. Conf. Elect. Comput. Eng.*, St. John's, NL, Canada, 2009, pp. 745–749.

[32] Y. Liang, Y. Zeng, E. Peh, and A. Hoang, "Sensing-throughput tradeoff for cognitive radio networks," *IEEE Trans. Wireless Commun.*, vol. 7, no. 4, pp. 1326–1337, Apr. 2008.

[33] A. Hawkes, "Spectra of some self-exciting and mutually exciting point processes," *Biometrika*, vol. 58, no. 1, pp. 83–90, 1971.

[34] Y. Ogata, "Statistical models for earthquake occurrences and residual analysis for point processes," *J. Amer. Stat. Assoc.*, vol. 83, no. 401, pp. 9–27, 1988.

[35] P. Reynaudbouret, V. Rivoirard, and C. Tuleaumalot, "Inference of functional connectivity in neurosciences via Hawkes processes," in *Proc. Global Conf. Signal Inf. Process.*, Austin, TX, USA, 2014, pp. 317–320.

[36] C. Luo, X. Zheng, and D. Zeng, "Inferring social influence and meme interaction with Hawkes processes," in *Proc. IEEE Int. Conf. Intell. Security Informat. (ISI)*, Baltimore, MD, USA, 2015, pp. 135–137.

[37] C. Guo and W. Luk, "Accelerating maximum likelihood estimation for Hawkes point processes," in *Proc. 23rd Int. Conf. Field Program. Logic Appl.*, Porto, Portugal, 2013, pp. 1–6.

[38] V. Veeravalli and P. Varshney, "Distributed inference in wireless sensor networks," *Philos. Trans.*, vol. 370, no. 1958, pp. 100–117, 2012.

[39] A. Aziz and N. Zaher, "C41. Multisensor estimate fusion based on Bayesian minimum mean square error criterion," in *Proc. 29th Nat. Radio Sci. Conf.*, Cairo, Egypt, 2012, pp. 503–514.

[40] Q. Yan and R. Blum, "Distributed signal detection under the Neyman–Pearson criterion," *IEEE Trans. Inf. Theory*, vol. 47, no. 4, pp. 1368–1377, May 2001.

[41] Y. Wu and W. Yang, "Optimal distributed decision fusion in the sense of the Neyman–Pearson test," in *Proc. Int. Conf. Radar*, Beijing, China, 2002, pp. 708–712.

[42] M. Moreira, "A conditional likelihood ratio test for structural models," *Econometrica*, vol. 71, no. 4, pp. 1027–1048, 2010.

[43] B. Aragam and Q. Zhou, "Concave penalized estimation of sparse Gaussian Bayesian networks," 2015. [Online]. Available: https://arxiv.org/abs/1401.0852.

[44] M. Zweig and G. Campbell, "Receiver-operating characteristic (ROC) plots: A fundamental evaluation tool in clinical medicine," *Clin. Chem.*, vol. 39, no. 4, pp. 561–577, 1993.

[45] J. Hanley and B. McNeil, "The meaning and use of the area under a receiver operating characteristic (ROC) curve," *Radiology*, vol. 143, no. 1, pp. 29–36, 1982.

[46] F. Schoonjans, "Presentation of receiver-operating characteristics (ROC) plots," *Clin. Chem.*, vol. 42, no. 1, pp. 986–987, 1996.

[47] K. B. Letaief and W. Zhang, "Cooperative communications for cognitive radio networks," *Proc. IEEE*, vol. 97, no. 5, pp. 878–893, May 2009.

[48] J. Traub and H. Wozniakowski, "Convergence and complexity of newton iteration for operator equations," *J. ACM*, vol. 26, pp. 250–258, Apr. 1979.

[49] X. Zhou, A. Hu, G. Li, L. Peng, Y. Xing, and J. Yu, "Design of a robust RF fingerprint generation and classification scheme for practical device identification," in *Proc. IEEE Conf. Commun. Netw. Security (CNS)*, Washington, DC, USA, 2019, pp. 196–204.

[50] L. Senigagliesi, M. Baldi, and E. Gambi, "Statistical and machine learning-based decision techniques for physical layer authentication," in *Proc. IEEE Global Commun. Conf. (GLOBECOM)*, Waikoloa, HI, USA, 2019, pp. 1–6.

[51] P. Zhang, T. Taleb, X. Jiang, and B. Wu, "Physical layer authentication for massive MIMO systems with hardware impairments," *IEEE Trans. Wireless Commun.*, vol. 19, no. 3, pp. 1563–1576, Mar. 2020.
[52] J. Zhang, Y. Li, T. Su, and X. He, "Quadratic FM signal detection and parameter estimation using coherently integrated trilinear autocorrelation function," *IEEE Trans. Signal Process.*, vol. 68, pp. 621–633, 2020, doi: 10.1109/TSP.2020.2965279.
[53] J. Tian, Y. Pei, Y. Huang, and Y. Liang, "Modulation-constrained clustering approach to blind modulation classification for MIMO systems," *IEEE Trans. Cogn. Commun. Netw.*, vol. 4, no. 4, pp. 894–907, Dec. 2018.
[54] A. Gritsenko, Z. Wang, T. Jian, J. Dy, K. Chowdhury, and S. Ioannidis, "Finding a 'new' needle in the haystack: Unseen radio detection in large populations using deep learning," in *Proc. IEEE Int. Symp. Dyn. Spect. Access Netw. (DySPAN)*, Newark, NJ, USA, 2019, pp. 1–10.

Zitong Liu received the B.S. degree in information engineering from the Nanjing University of Aeronautics and Astronautics, Nanjing, China, in 2019, where she is currently pursuing the M.S. degree with the College electronic information engineering. Her research interests include data analytics, wireless communications, and cognitive radio networks.

Guoru Ding (Senior Member, IEEE) received the B.S. degree (Hons.) in electrical engineering from Xidian University, Xi'an, China, in 2008, and the Ph.D. degree (Hons.) in communications and information systems from the College of Communications Engineering, Nanjing, China, in 2014.

He is currently an Associate Professor with the College of Communications Engineering, Army Engineering University. From 2015 to 2018, he was a Postdoctoral Research Associate with the National Mobile Communications Research Laboratory, Southeast University, Nanjing, China. His research interests include cognitive radio networks, massive MIMO, machine learning, and data analytics over wireless networks. He has received the Excellent Doctoral Thesis Award of the China Institute of Communications in 2016, the Alexander von Humboldt Fellowship in 2017, the Excellent Young Scientist of Wuwenjun Artificial Intelligence in 2018, and the 14th IEEE COMSOC Asia–Pacific Outstanding Young Researcher Award in 2019. He was a recipient of the Natural Science Foundation for Distinguished Young Scholars of Jiangsu Province, China, and six best paper awards from international conferences, such as the IEEE VTC-FALL 2014. He has served as a Guest Editor for the IEEE JOURNAL ON SELECTED AREAS IN COMMUNICATIONS (special issue on spectrum sharing and aggregation in future wireless networks). He is currently an Associate Editor of the IEEE TRANSACTIONS ON COGNITIVE COMMUNICATIONS AND NETWORKING and a Technical Editor of the IEEE 1900.6 Standard Association Working Group.

Zheng Wang (Member, IEEE) received the B.S. degree in electronic and information engineering from the Nanjing University of Aeronautics and Astronautics (NUAA), Nanjing, China, in 2009, the M.S. degree in communications from the Department of Electrical and Electronic Engineering, University of Manchester, Manchester, U.K., in 2010, and the Ph.D. degree in communication and signal processing from Imperial College London, U.K., in 2015.

From 2015 to 2016, he served as a Research Associate with Imperial College London. From 2016 to 2017, he was an Senior Engineer with Radio Access Network Research and Development Division, Huawei Technologies Company. He is currently an Associate Professor with the College of Electronic and Information Engineering, NUAA. His current research interests include lattice methods for wireless communications, MIMO systems, machine learning, and physical layer security.

Shilian Zheng (Member, IEEE) received the B.S. degree in telecommunication engineering and the M.S. degree in signal and information processing from Hangzhou Dianzi University, Hangzhou, China, in 2005 and 2008, respectively, and the Ph.D. degree in communication and information system from Xidian University, Xi'an, China, in 2014.

He is currently an Associate Researcher with Science and Technology on Communication Information Security Control Laboratory, Jiaxing, China. He holds more than ten patents. His research interests include cognitive radio, spectrum management, compressed sensing, and deep learning based radio signal processing.

Jiachen Sun received the B.S. degree in information engineering from Southeast University in 2016, the M.S. degree in communication engineering from Army Engineering University, Nanjing, China, in 2018. She is currently pursuing the Ph.D. degree with the College of Communications Engineering, Army Engineering University of PLA, Nanjing. Her research interests include data analytics, wireless communications, and cognitive radio networks.

Qihui Wu (Senior Member, IEEE) received the B.S. degree in communications engineering, and the M.S. and Ph.D. degrees in communications and information systems from the Institute of Communications Engineering, Nanjing, China, in 1994, 1997, and 2000, respectively. He was appointed the Changjiang Distinguished Professorship in 2016. From 2003 to 2005, he was a Postdoctoral Research Associate with Southeast University, Nanjing. From 2005 to 2007, he was an Associate Professor with the Institute of Communications Engineering, PLA University of Science and Technology, Nanjing, where he is currently a Full Professor. From March 2011 to September 2011, he was an Advanced Visiting Scholar with the Stevens Institute of Technology, Hoboken, USA. Since 2016, he has been with the Nanjing University of Aeronautics and Astronautics and appointed as a Distinguished Professor. His current research interests span the areas of wireless communications and statistical signal processing, with emphasis on system design of software defined radio, cognitive radio, and smart radio.